BIOMOLECULES
& THERAPEUTICS

Systematic Target Screening Revealed That Tif302 Could Be an Off-Target of the Antifungal Terbinafine in Fission Yeast

Sol Lee[1], Miyoung Nam[1], Ah-Reum Lee[1], Jaewoong Lee[1], Jihye Woo[1], Nam Sook Kang[1], Anand Balupuri[1],
Minho Lee[2], Seon-Young Kim[3], Hyunju Ro[4], Youn-Woong Choi[5], Dong-Uk Kim[6,*] and Kwang-Lae Hoe[1,*]

[1]*Department of New Drug Development, Chungnam National University, Daejeon 34134,*
[2]*Department of Life Science, Dongguk University-Seoul, Goyang 10326,*
[3]*Personalized Genomic Research Center, Korea Research Institute of Bioscience & Biotechnology (KRIBB), Daejeon 34141*
[4]*Department of Biological Science, College of Bioscience & Biotechnology, Chungnam National University, Daejeon 34134,*
[5]*Korea United Pharm. Inc., Seoul 06116,*
[6]*Rare Disease Research Center, Korea Research Institute of Bioscience & Biotechnology (KRIBB), Daejeon 34141, Republic of Korea*

Abstract

We used a heterozygous gene deletion library of fission yeasts comprising all essential and non-essential genes for a microarray screening of target genes of the antifungal terbinafine, which inhibits ergosterol synthesis via the Erg1 enzyme. We identified 14 heterozygous strains corresponding to 10 non-essential [7 ribosomal-protein (RP) coding genes, *spt7*, *spt20*, and *elp2*] and 4 essential genes (*tif302*, *rpl2501*, *rpl31*, and *erg1*). Expectedly, their *erg1* mRNA and protein levels had decreased compared to the control strain SP286. When we studied the action mechanism of the non-essential target genes using cognate haploid deletion strains, knockout of SAGA-subunit genes caused a down-regulation in *erg1* transcription compared to the control strain ED668. However, knockout of RP genes conferred no susceptibility to ergosterol-targeting antifungals. Surprisingly, the RP genes participated in the *erg1* transcription as components of repressor complexes as observed in a comparison analysis of the experimental ratio of *erg1* mRNA. To understand the action mechanism of the interaction between the drug and the novel essential target genes, we performed isobologram assays with terbinafine and econazole (or cycloheximide). Terbinafine susceptibility of the *tif302* heterozygous strain was attributed to both decreased *erg1* mRNA levels and inhibition of translation. Moreover, Tif302 was required for efficacy of both terbinafine and cycloheximide. Based on a molecular modeling analysis, terbinafine could directly bind to Tif302 in yeasts, suggesting Tif302 as a potential off-target of terbinafine. In conclusion, this genome-wide screening system can be harnessed for the identification and characterization of target genes under any condition of interest.

Key Words: Antifungal, Terbinafine, Drug target, Ribosomal protein, Sterol, Translation

INTRODUCTION

To bridge the gap between drug discovery and development, the characterization of drug targets has been a long-thought goal (Kramer and Cohen, 2004; Schenone *et al.*, 2013). The identification of potential off-targets would aid in the development of safer and more efficacious drugs (Parsons *et al.*, 2006; Schenone *et al.*, 2013), even after a relevant on-target is well established. Recent advances in genomic technologies have made it possible to systematically screen drug targets *in vivo* by employing diverse model organisms, such as yeasts (Winzeler *et al.*, 1999; Kim *et al.*, 2010), nematodes, fruit flies, and zebrafish (Kramer and Cohen, 2004; Housden *et al.*, 2017). When the gene dosage of drug target genes is reduced to a half by a variety of methods, such as gene deletion, siRNA, and CRISPR technique, then, by the principle of drug-induced haploinsufficiency, the growth profile is affected in response to a drug treatment due to lower copy number of target genes (Giaever *et al.*, 1999). Genome-wide target screening is culminating with the advent of the CRISPR/Cas9

technology in human cell lines (Shalem *et al*., 2014).

We have constructed a genome-wide gene deletion library with built-in bar codes in a gene-specific manner in fission yeast (Winzeler *et al*., 1999; Kim *et al*., 2010), following budding yeast (Winzeler *et al*., 1999). In yeasts, the availability of gene-specific bar codes has enabled the detection of target genes affected under any condition of interest in a systematic way (Kim *et al*., 2010). As a pioneering study, 78 therapeutic compounds were used in the heterozygous budding yeast gene deletion library to reveal the modes of action of several drugs (Lum *et al*., 2004). However, widespread applications of the technique have been hampered due to difficulties in elucidating the action mechanisms of screened target genes. For example, many target genes correspond to RPs, transcriptional regulators, and signaling molecules, whose functions are yet to be elucidated (Lum *et al*., 2004; Han *et al*., 2013). To circumvent this difficulty, previous screenings have utilized a haploid gene deletion library (Parsons *et al*., 2006). In this case, loss-of-function assays make in-depth studies easier to reveal their action mechanisms, because the relevant target gene is null in haploids (knockout), unlike haploinsufficiency (knockdown) in heterozygotes. Nonetheless, it is still preferable to use a heterozygous deletion library covering essential and non-essential genes, as essential genes are the ideal targets of pathogens (Ianiri and Idnurm, 2015; Rancati *et al*., 2018) and most eukaryotic organisms exist as diploid (2N).

Despite the recent advent of the cutting-edge CRISPR technology, the yeast screening system remains useful because of easier genetic handling and bar code detection. Since yeasts are classified as fungi, the yeast model system would be the best choice for screening of antifungals (Sipiczki, 2000). Terbinafine (TRB) has been developed as the first oral antimycotic in the allylamine class (Ostrosky-Zeichner *et al*., 2010), and its action mechanism is based on inhibiting squalene epoxidase (Erg1) in the ergosterol synthesis pathway. Thus, TRB causes ergosterol depletion, which is critical for membrane integrity and growth in fungi (Ryder, 1992). Moreover, inhibition of Erg1 leads to the intracellular accumulation of squalene, a toxic metabolite that leads to rapid cell death (Darkes *et al*., 2003). We chose TRB as a test drug out of several antifungals, since TRB is much more effective in fission yeast, compared to budding yeast (Lum *et al*., 2004; Cokol *et al*., 2011). Previously, a set of TRB target genes were identified from the haploid deletion library of fission yeast (Fang *et al*., 2012).

In this study, we identified target genes of TRB using the heterozygous gene deletion library and characterized the action mechanisms of the screened target genes as a proof-of-concept that supports harnessing this genome-wide screening system for the identification and characterization of target genes affected under any condition of interest.

MATERIALS AND METHODS

Chemicals and reagents

All chemicals and reagents were obtained from Sigma-Aldrich (St Louis, MO, USA), unless stated otherwise. Yeast extract and agar were purchased from BD Difco (Sparks, MD, USA). TRB was provided by Korea United Pharm. Inc (Seoul, Korea). All oligonucleotides were purchased from Bioneer (Daejeon, Korea).

Fission yeast gene deletion library and strains

For the systematic screening of TRB target genes in fission yeast, we used the heterozygous gene deletion library (2N) constructed in a previous study (Kim *et al*., 2010). In brief, deletion cassettes containing a pair of unique molecular bar codes (up- and down-tag) were generated and transformed into the diploid SP286 strain (h^+/h^+; *ade*6-M210/*ade*6-M216, *leu*1-32/*leu*1-32, *ura*4-D18/*ura*4-D18) using the *KanMX* gene as a selection marker. Heterozygous gene deletion strains were constructed by homologous recombination of the deletion cassettes, and then selected on YES (0.5% yeast extract, 3% glucose, and appropriate amino acid supplements) plates containing 100 μg/mL G418 (Duchefa Biochemie, Haarlem, Netherlands). The deletion library consisted of 1,260 essential genes and 3,576 non-essential genes, representing 98.4% (4,836/4,914) of all protein-coding genes.

For the loss-of-function analyses of non-essential genes, cognate haploid gene deletion strains (1N) were derived from heterozygous gene deletion strains, if available. The ED668 strain (h^+; *ade*6-M216, *leu*1-32, *ura*4-D18) was used as a haploid control. Fission yeast cells were cultivated in complete YES medium at 28ºC unless stated otherwise. All strains used in this study are available from Bioneer.

Screening of target genes by microarray and spotting assay

The genome-wide screening of TRB target genes was performed via microarrays, as previously reported (Kim *et al*., 2010; Han *et al*., 2013) with slight modifications. Microarray screening was performed using a custom-made GeneChip (48K KRIBB_SP2; Thermo Fisher Scientific, Waltham, MA, USA) and fluorescence-labeled probes were prepared by amplification of the unique molecular bar codes. Through 2 independent microarray experiments, heterozygous target strains were selected by the criterion of relative growth fitness of <0.94 (p<0.05), compared with the untreated sample. The primarily screened target strains were confirmed using spotting assays, based on individual growth fitness. For the spotting assay, cells in log phase were diluted to an OD_{600}=0.5 in YES media and spotted in 5-fold serial dilutions onto YES agar plates with or without drugs. The heterozygous target strains were, then, classified by their extent of susceptibility against TRB, as follows: severe (SSS) when growth fitness decreased by more than 2 serial dilutions (>25-fold susceptibility); moderate (SS), between 1 to 2 serial dilution(s) (5-25-fold susceptibility); and mild (S), less than 1 serial dilution (<5-fold susceptibility). The relevant TRB target genes were then subjected to GO analysis using the Gene Ontology Resource (http://geneontology.org/).

Measurement of *erg1* mRNA levels using RT-PCR

To measure *erg1* mRNA levels of target strains, cells were cultivated until log phase was reached in YES media, harvested using conical tubes, and subjected to RT-PCR. In brief, mRNA was extracted using TRIzol reagent (Thermo Fisher Scientific) and reverse transcribed to cDNA using the Quantiscript Reverse Transcriptase (Qiagen, Hilden, Germany). cDNA (100 ng) was then amplified using iQ SYBR Green Supermix, and measured on a CFX Connect™ Real-Time PCR Detection System (Bio-Rad Laboratories, Hercules, CA, USA). Actin was used as an endogenous control for normalization. The primer sequences were as follows: *erg1*: forward, 5′-CGCTATATGAAGGCTCTT-GAATCG-3′ and reverse, 5′-GATGAGAAGGGCTATGGTCTA-

AAC-3′; *act1*: forward, 5′-TCCAACCGTGAGAAGATGACT-3′ and reverse, 5′-CGACCAGAGGCATACAAAGAC-3′.

Determination of squalene levels using HPLC

Intracellular squalene levels were measured as previously described (Takami *et al*., 2012) with slight modifications. In brief, cells were cultured in conical tubes in the presence of 150 nM TRB. Approximately, $2×10^8$ cells were washed twice with ultrapure water and resuspended in a 1 mL mixture of extract solvent [chloroform/methanol, 2:1 (v/v)] and glass beads (diameter=0.4-0.6 mm). The samples were lysed by sonication for 10 min and mixed overnight. The supernatant was harvested by centrifugation at 16,110×*g* for 5 min and dried by evaporation for 30 min using a centrifugal vacuum evaporator. From the dried supernatant, squalene was extracted using 50 μL of 100% methanol. The amount of squalene was analyzed by using an acetonitrile: acetone (60:40, v/v) mobile phase, Agilent 1260 HPLC (Agilent Technologies, Santa Clara, CA, USA), and a YMC column (product no. JH08S04-2546WT; YMC, Kyoto, Japan) at a flow rate of 1 mL/min at room temperature. The amount of intracellular squalene was detected by measuring the A_{220}. For generating a standard curve, 4 different concentrations of squalene (10, 50, 100, and 150 ppm) were used.

Comparison of relative drug sensitivity using pattern map

To compare the relative drug sensitivity of target strains over control strains (SP286 for heterozygous and ED668 for haploid gene deletion strains), a sensitivity pattern map was employed by visualization of the relative sensitivity data from spotting assays, using a heat map. When the target strains showed no, mild (S,<5-fold), moderate (SS, 5-25-fold), or severe (SSS,>25-fold) susceptibility compared with the control strains, the relative drug sensitivity was represented in blue, light blue, light red, or red on the heat map, respectively.

Assessment of drug-drug target interactions using isobologram assay

To assess drug-drug target interactions by co-treatments of the heterozygous target strains with TRB and the other drug (ECZ or CHX), isobologram analysis was performed as previously described with slight modifications (Chou, 2006). In brief, IC_{50} values of a pair of drugs were determined individually in each target strain using 96 deep-well plates, and the IC_{50} values of drugs were plotted at *x* and *y* axes, respectively. A diagonal line was drawn between the pair of IC_{50} spots, representing the line of additivity as a control. Next, each target strain was co-treated with various concentrations of TRB and ECZ (or CHX). Several data sets corresponding to the same IC_{50} were then obtained and plotted on the graph. When the dots are located below, on, or above the diagonal line, the results indicate synergy, additivity, or antagonism, respectively.

Complementation analysis

For the complementation test, the *erg1* or *tif302* gene was ectopically expressed in the *Δtif302/tif302* heterozygous strain under the nmt1 promoter in the pREP4X vector. The expression plasmid was transformed using the lithium acetate method and incubated on YES agar plates containing the selection marker nourseothricin (catalog no. 2882; BioVision Inc, Milpitas, CA, USA). Growth fitness of the transformants was analyzed on YES agar plates containing 30 nM TRB using

the spotting assay, and their relative fitness was compared with the SP286 control or *Δtif302/tif302* heterozygous strain containing the empty vehicle plasmid. TRB sensitivity was quantified using densitometry and Image J (National Institute of Health, Bethesda, MD, USA).

Molecular modeling

As a first step of molecular modeling, protein databank (PDB) data were retrieved from RCSB PDB (https://www.rcsb.org/) and all amino acid sequence data were retrieved from the UniProt database (http://www.uniprot.org) as follows: human SQLE (ortholog of yeast Erg1, 574 amino acids), PDB code: 6C6P, UniProt ID: Q14534; human EIF3B (814 amino acids), PDB code: 5K1H, UniProt ID: P55884; budding yeast Erg1p (496 amino acids), UniProt ID: P32476; budding yeast Prt1p (ortholog of fission yeast Tif302, 763 amino acids), PDB code: 4U1F, UniProt ID: P06103; fission yeast Erg1 (457 amino acids), UniProt ID: Q9C1W3; fission yeast Tif302 (725 amino acids), UniProt ID: Q10425. After obtaining the amino acid sequences of interest, they were aligned to one another via BLAST (https://blast.ncbi.nlm.nih.gov/Blast.cgi/). Using the available crystal structures, including the human SQLE, human EIF3B, and budding yeast Prt1p proteins as templates, unknown protein structures of interest, such as fission yeast Erg1 and Tif302 and budding yeast Erg1p were built via homology modeling using MODELER version 9.20 in Discovery Studio 2019 (BIOVIA, San Diego, CA, USA). Docked binding modes were obtained using the homology structure models. Among several homology structure models, the best one was selected based on the lowest probability density function (PDF) total energy and discrete optimized protein energy (DOPE) scores. The AutoDock 4.2.6 (The Scripps Research Institute, La Jolla, CA, USA) was then employed for molecular docking to assess the interactions between TRB and potential binding sites of homology structure models. The three dimensional (3D) structure of proteins and TRB was processed using AutoDock Tools 1.5.6. AutoGrid program (The Scripps Research Institute) was used for generating 3D affinity grid fields with a grid size and spacing of 40×40×40 $Å^3$ and 0.375 Å, respectively. A total of 100 docking runs, $25×10^5$ energy evaluations, and 27,000 iterations were carried out using the Lamarckian genetic algorithm method. For more details, see the supplementary material.

Statistical analysis

All experiments were analyzed using triplicate samples and repeated at least 3 times. Data are presented as the mean ± SD, unless indicated otherwise. Statistical comparisons between groups were performed using Student's *t*-test. Results with *p*-values <0.05 were considered statistically significant.

RESULTS

Microarray screening of TRB target genes using the heterozygous gene deletion library in fission yeast

Through the primary microarray screening and secondary spotting assay against TRB, we identified 24 heterozygous target strains corresponding to 7 essential and 17 non-essential genes (Supplementary Table 1). According to GO analysis of the relevant target genes in terms of biological process, 14 genes encoding mostly ribosomal proteins were related

to 'translation' with a significant (p<2.78E-14) enrichment of 13 fold. The remaining 10 genes were related to 'transport' (4 non-essential), 'transcription' (3 non-essential), and 'miscellaneous' (3 essential genes including *erg1*). The systematic TRB target screening was proven successful as the well-known TRB target (Ryder, 1992), the *erg1* gene which encodes squalene epoxidase was identified in the screening.

For further in-depth functional studies, we narrowed down the number of TRB target strains to 14 (10 non-essential and 4 essential genes) by using a cut-off of severe susceptibility (i.e., SSS), as shown in Table 1. According to GO analysis in terms of biological process, except for the well-known *erg1*, the remaining 13 target genes were found to be related to the following 2 types of biological processes: 'translation' (3 essential genes: *tif302*, *rpl2501*, and *rpl31*; 7 non-essential genes:

rps2402, *rps2801*, *rps1002*, *rps1601*, *rps1802*, *rps1901*, and *rpl1602*) and 'transcription' (3 non-essential genes: *spt7*, *spt20*, and *elp2*). Null mutation of the 10 TRB target genes resulted in abnormal morphologies when the haploid gene-deletion mutants were microscopically observed for several generations after germination (Hayles *et al*., 2013). Furthermore, all the target genes were found to be associated with diverse human diseases, such as Diamond-Blackfan anemia (DBA) and cancers (see Table 1). So far, at least 19 genes have been reported to cause DBA by haploinsufficiency, and most DBA-associated genes encode RPs (Ulirsch *et al*., 2018). Human orthologs of the 5 TRB target genes were found to be associated with DBA, and all of them encode RPs.

Table 1. List of the top 14 terbinafine targets

Gene name	Gene description[a]	GO[b]	Dispensability[c] (Susceptibility[d])	Morphology[e]	Disease relationship[f]
erg1	Squalene monooxygenase	Ergosterol Synthesis	E (SSS)	Misshapen	Neuro cancer (Mahoney *et al*., 2019), Hepatocarcinoma (Sui *et al*., 2015)
tif302	Translation IF3b	Translation	E (SSS)	No germination	Bladder, prostate cancer (Wang *et al*., 2013)
rpl2501	60S RP L25		E (SSS)	Rounded	Rheumatoid arthritis (Ito *et al*., 2014)
rpl31	60S RP L31		E (SSS)	Limited cell division	*DBA (Farrar *et al*., 2014; Ulirsch *et al*.. 2018) [617415][g]
rps2402	40S RP S24		NE (SSS)	Wild type	*DBA (Gazda *et al*., 2006; Ulirsch *et al*., 2018) [610629][g]
rps2801	40S RP S28		NE (SSS)	Wild type	*DBA (Gripp *et al*., 2014; Ulirsch *et al*., 2018) [606164][g]
rps1002	40S RP S10		NE (SSS)	Wild type	*DBA (Doherty *et al*., 2010; Ulirsch *et al*., 2018) [613308][g]
rps1601	40S RP S16		NE (SSS)	Long	Melanoma, colon cancer (Zinzalla *et al*., 2011)
rps1802	40S RP S18		NE (SSS)	Misshapen	Colorectal cancer (Takemasa *et al*., 2012)
rps1901	40S RP S19		NE (SSS)	Long	*DBA (Draptchinskaia *et al*., 1999; Ulirsch *et al*., 2018) [105650][g]
rpl1602	60S RP L13/L16		NE (SSS)	Wild type	Inflammatory disorder (Mukhopadhyay *et al*., 2008)
spt7	SAGA subunit	Transcription	NE (SSS)	Long branched	Mycosis fungoides (Dong *et al*., 2018)
spt20	SAGA subunit		NE (SSS)	Long branched	Myeloid neoplasms (Visconte *et al*., 2017)
elp2	RNAP II elongator subunit		NE (SSS)	Long	Mental retardation (Cohen *et al*., 2015) [617270][g]

[a]Gene description is as indicated in PomBase (https://www.pombase.org/).
[b]GO analysis has been analyzed in terms of biological process using the Gene Ontology Resource (http://geneontology.org/). Unless available, the GO term of PomBase was used.
[c]Dispensability data was obtained from the previous study (Kim *et al*., 2010) and tetrad analysis in this study. E, essential genes; NE, Non-essential genes.
[d]SSS represents severe susceptibility against terbinafine.
[e]Morphology data was previously reported from the previous (Hayles *et al*., 2013) and the studies.
[f]Genetic disorders were identified in OMIM (https://www.omim.org/) or pubmed (https://pubmed.ncbi.nlm.nih.gov/).
[g]When genetic disorders were identified in OMIM, their MIM numbers are represented by the square bracket.
*DBA is short for Diamond–Blackfan anemia.

All heterozygous TRB target strains are associated with decreased levels of *erg1* mRNA and Erg1 protein

Considering that the 14 heterozygous targets were identified by virtue of the TRB-induced haploinsufficiency, their cellular levels of *erg1* mRNA or Erg1 protein should be lower than the diploid control SP286. As expected, all heterozygous target strains showed significantly ($p<0.05$) lower levels of *erg1* mRNA, ranging from 30-80% of SP286 when measured prior to TRB treatment (Fig. 1A). Next, we assessed the levels of squalene, which is a substrate of Erg1, as a secondary readout of Erg1 protein levels (Fig. 1B). Squalene levels in the SP286 control strain were too low to detect under the normal condition prior to TRB treatment. However, TRB treatment (150 nM for 18 h) of all heterozygous target strains resulted in a significant ($p<0.05$) induction of squalene levels by 2-10 fold compared to SP286. Notably, the *tif302* and *erg1* strains showed a higher induction fold in squalene levels.

If all target strains had lower levels of *erg1* mRNA and Erg1 protein, they would also be susceptible to similar classes of antifungals targeting ergosterol synthesis. To assess this possibility, all target strains were treated with antifungals targeting ergosterol synthesis, including tolnaftate (TFT, thiocarbamate class targeting Erg1) (Ryder *et al*., 1986), econazole (ECZ), and miconazole (MCZ, azole class targeting Erg11, downstream of Erg1) (Ostrosky-Zeichner *et al*., 2010), as well as TRB (allylamine class targeting Erg1), and their susceptibility was compared with drugs and chemicals not targeting ergosterol synthesis, including diethylstilbestrol (DES, steroid medication for breast cancer), cycloheximide (CHX, targeting

translation elongation in eukaryotic cells), H_2O_2 (ROS stress), and MMS (mutagen) (Fig. 1C). According to the sensitivity pattern map, which compares the TRB target strains with the SP286 control and 10 random heterozygous strains, all of the TRB target strains showed higher susceptibility only towards antifungals that target ergosterol synthesis and not towards chemicals that do not target ergosterol synthesis. Intriguingly, the steroid drug DES and translation inhibitor CHX also showed a pattern map similar to ergosterol-targeting antifungals in TRB target strains, suggesting that their action mechanism related to the modulation of ergosterol levels. For example, DES would act as an ergosterol analogue because of its similar chemical structure to ergosterol (Korach *et al*., 1978).

Taken together, the results indicate that the sensitivity of all heterozygous TRB targets strains screened under the principle of drug-induced haploinsufficiency is attributed to decreased levels of *erg1* mRNA and Erg1 protein.

Among the cognate haploid deletion strains, deletion haploids of SAGA-subunit genes are also susceptible to TRB, but deletion haploids of RP genes are not

When the relevant genes of heterozygous target strains were non-essential, their cognate haploid deletion strains were employed for elucidation of molecular mechanism through loss-of-function (knockout) analysis. Out of the 10 heterozygous target strains of non-essential genes, 9 cognate haploid strains corresponding to 7 RP and 2 SAGA-subunit genes, except for *elp2*, were available for further studies.

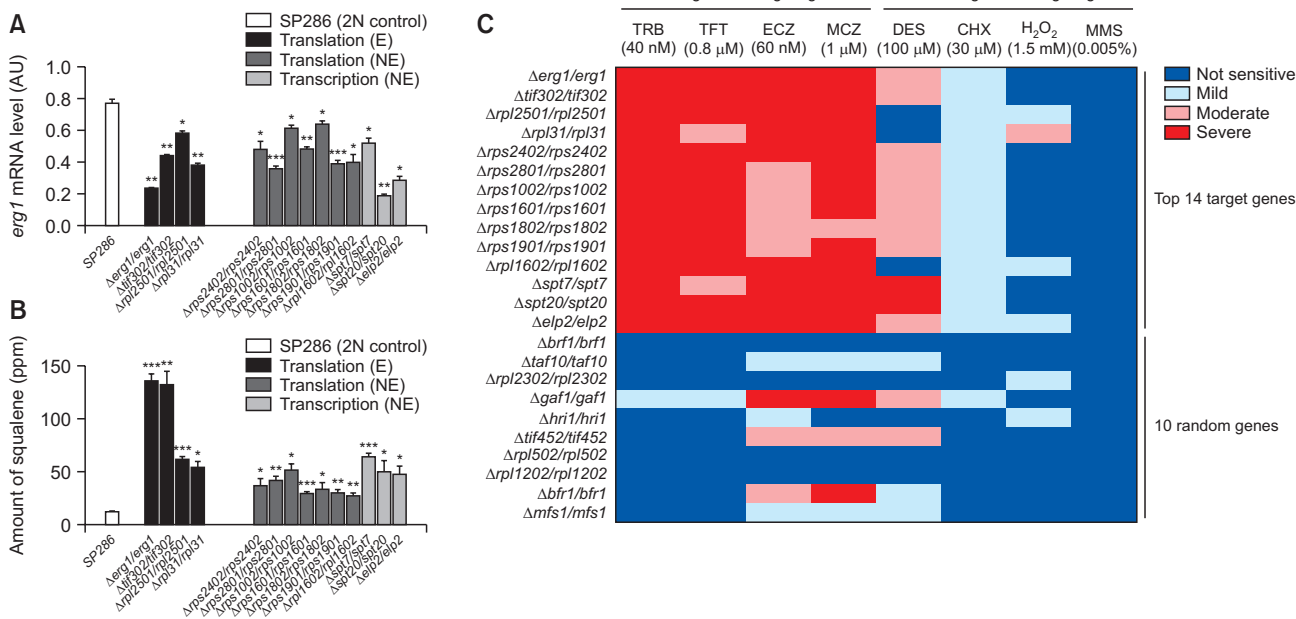To check whether the TRB-induced haploinsufficiency in

Fig. 1. Functional analyses of the 14 heterozygous TRB target strains. (A) The *erg1* mRNA levels without TRB treatment were measured by using RT-PCR and normalized over *act1*. (B) The squalene levels after TRB treatment were determined by using HPLC. The bars were filled with various brightness of black color to represent the GO term and dispensability of each heterozygous deletion strain, as indicated on the insets. *n*=3; *$p<0.05$, **$p<0.01$, or ***$p<0.001$ vs. SP286. (C) The relative susceptibility in response to the indicated drugs or toxic chemicals compared with SP286 was assessed using spotting assays and visualized as a pattern map. The heterozygous deletion strains of 10 random genes were used as controls. The extent of relative susceptibility is represented as indicated on the inset. Severe (>25-fold), moderate (5-25-fold), mild (<5-fold), and not susceptible; terbinafine (TRB), tolnaftate (TFT), econazole (ECZ), miconazole (MCZ), diethylstilbesterol (DES), cycloheximide (CHX), and methyl methanesulfonate (MMS).
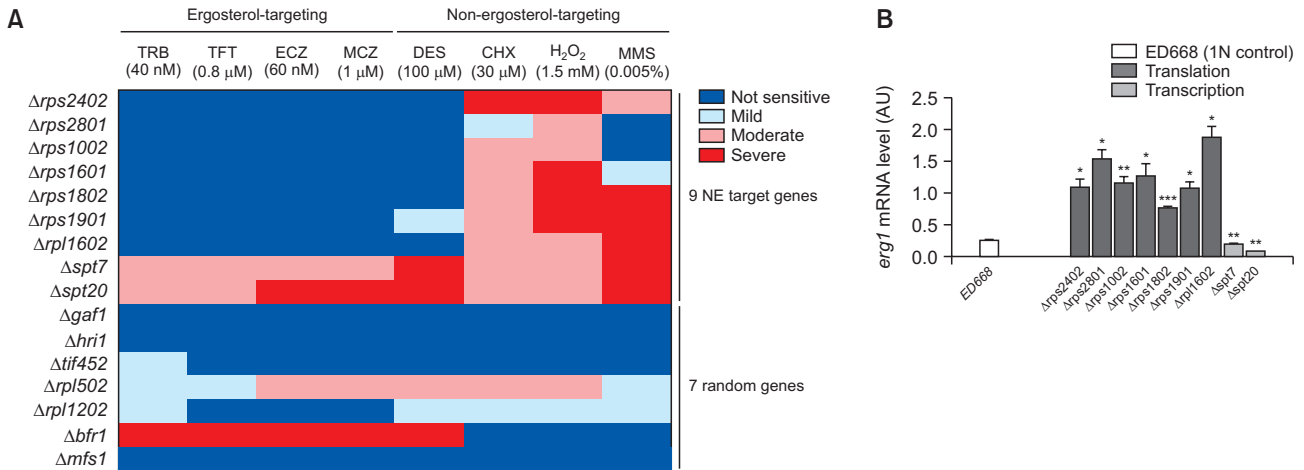
Fig. 2. Functional analyses of the 9 haploid TRB target strains. (A) For loss-of-function analysis, the haploid deletion strains were retrieved from their cognate heterozygous TRB target strains when their relevant genes were non-essential. Their relative susceptibility in response to the indicated drugs or toxic chemicals compared with ED668 was assessed by using spotting assays, and visualized as a pattern map. The haploid deletion strains of 7 random genes were used as controls. The extent of relative susceptibility is represented as indicated on the inset. Severe (>25-fold), moderate (5-25-fold), mild (<5-fold), and not susceptible; terbinafine (TRB), tolnaftate (TFT), econazole (ECZ), miconazole (MCZ), diethylstilbesterol (DES), cycloheximide (CHX), and methyl methanesulfonate (MMS). (B) The *erg1* mRNA levels without TRB treatment were measured by using RT-PCR and normalized over *act1*. The bars were filled with various brightness of black color to represent the GO term of each haploid deletion strain, as indicated on the insets. $n=3$; *$p<0.05$, **$p<0.01$, or ***$p<0.001$ vs. ED668.

the heterozygous target strains would reproduce in the cognate haploid deletion strains, we performed the sensitivity pattern map analysis with the 9 available haploid deletion strains against the same set of drugs used with the heterozygous target strains (Fig. 1A) by using the ED668 and 7 deletion haploids of random genes as controls (Fig. 2A). Surprisingly, compared with the controls, none of the 7 haploid deletion strains of RP genes showed susceptibility against the antifungals targeting ergosterol synthesis, whereas the 2 haploid deletion strains of SAGA-subunit genes (*spt7* and *spt20*) did. In contrast, most cognate haploid deletion strains showed susceptibility against chemicals and drugs not targeting ergosterol synthesis, compared with the haploid deletion controls of random genes.

To elucidate underlying mechanisms of the above phenomenon, first *erg1* mRNA levels of the 9 haploid deletion strains were measured without TRB treatment (Fig. 2B). Although all the heterozygous target strains showed significantly ($p<0.05$) decreased levels of *erg1* mRNA compared with SP286 (Fig. 1A), all the 7 deletion haploids of RP genes showed significantly ($p<0.05$) increased levels by 3-6 folds compared with the ED668 haploid control. In contrast, the 2 deletion haploids of SAGA-subunit genes showed significantly ($p<0.01$) decreased levels, as like their corresponding heterozygotes. Taken together, knockout of the SAGA-subunit genes conferred TRB susceptibility to the haploid deletion strains because of the decreased levels of *erg1* mRNA. Consistently, SAGA subunits have been reported to be transcriptional co-activators of ergosterol biosynthetic genes (Hickman *et al*., 2011; Dewhurst-Maridor *et al*., 2017). On the other hand, knockout of the RP genes did not confer TRB susceptibility to the haploid deletion strains, because of increased levels of *erg1* mRNA. Probably, the perturbation of *erg1* mRNA in the 9 cognate deletion haploids was associated with their susceptibility against the non-ergosterol targeting chemicals and drugs.

The RPs can work as components of suppressor complexes for the *erg1* transcription

The above results prompted us to elucidate the underlying action mechanism. The clue for the answer came from the experimental ratios of *erg1* mRNA levels observed in the 4 different kinds of test strains (as shown in the box on top of Fig. 3; see Supplementary Table 2 for the experimental datasets).

As the first step to answer, we applied 3 speculations based on the experimental ratios of *erg1* mRNA levels of the 4 test strains: (i) the role of RPs should be associated with transcription factors because their presence or absence affected the transcription levels of *erg1* mRNA. In accordance, dozens of ribosome-free RPs have been reported to play roles in cell growth by acting as transcription regulators, besides their classical roles in ribosome assembly (Torres *et al*., 2001; Warner and McIntosh, 2009; Zhou *et al*., 2013, 2015). (ii) The RPs should serve as repressors of *erg1* transcription, rather than activators, to fit the situation observed in the haploid strains (1N); the absence of RPs in the haploid deletion strains ED668-ΔRP (no. of RP gene=0) upregulated *erg1* mRNA compared with ED668 (no. of RP gene=1). Indeed, the ED668-ΔRP strain showed a higher ratio of *erg1* mRNA (4.2) than the ED668 control strain (1.0). (iii) The RPs should work as components of repressor complexes rather than conventional repressor monomers in a stoichiometry-dependent manner to explain the paradoxical situation in the diploid strains (2N); the more RP, the higher the *erg1* mRNA levels. Indeed, the SP286 diploid control strain (no. of RP gene=2) showed a higher ratio of *erg1* mRNA (2.7) than that of SP286-ΔRP/RP (1.6) (no. of RP gene=1). According to the gene balance theory (Jallepalli and Pellman, 2007; Veitia and Potier, 2015), the functional numbers of repressor complexes would be determined by the stoichiometry among components, rather than by nominal numbers of repressors. The stoichiometry among components can be determined such as 3 RP: 2 protein A: 2 protein B, as long as it fits the experimental ratios of *erg1* mRNA of each
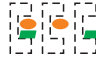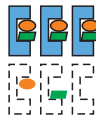
Experimental ratio of *erg1* mRNA	1.0	4.2	2.7	1.6

Model		Ploidy	Haploid (1N)		Diploid (2N)	
		Strain	ED668	ED668-ΔRP	SP286	SP286-ΔRP/RP
Speculation	No. of RP gene		1	0	2	1
	Stoichiometry		Repressor complex / Ribosomal protein / Protein A / Protein B — 3 : 2 : 2			
	No. of repressor (a)		1	0	2	3
Correction	No. of *erg1* gene (b)		1	1	2	2
	Dilution factor (c)		1	1	1.6	1.6
Final no. of repressor (a/b/c)			1	0	0.6	0.9

Fig. 3. The proposed model for the action mechanism of the 7 non-essential RP genes. The 4 test strains harbor the indicated number of RP genes depending on their ploidy and deletion status. Note that RP should serve as components of repressor complexes for *erg1* transcription, as speculated by the experimental ratio of their *erg1* mRNA levels (on the top box). In turn, the number of repressors (a) is determined by the considering the stoichiometry among components, as indicated. After corrections considering the copy number of *erg1* gene (b) and dilution factor due to different cellular volumes (c), the final number of repressors is calculated by the equation of a/b/c (on bottom), which is in a reverse order compared with that of the experimental ratio of *erg1* mRNA.

test strain. In this regard, the ratio of 2:1 (SP286: SP286-ΔRP/RP) for the nominal number of RPs was fixed as a 2:3 ratio for the functional number of repressor complexes.

Next, we took a couple of corrections into consideration to get the final numbers of repressor complexes: (i) the number of functional repressor complexes should be corrected based on a unit number of *erg1* gene to normalize different *erg1* gene numbers, depending on ploidy. (ii) Additionally, the dilution ef-

fects should be considered because of different cellular volumes depending on ploidy. Generally, the volume of diploid strains has been reported to be 1.6 times as large as that of haploid strains (Weiss *et al.*, 1975). Through the speculations and corrections, the final number of repressor complexes was determined as shown in the bottom line of Fig. 3, which fits into the experimental ratio of *erg1* mRNA (inside the box, on top) in the reverse order. The proposed model suggests that
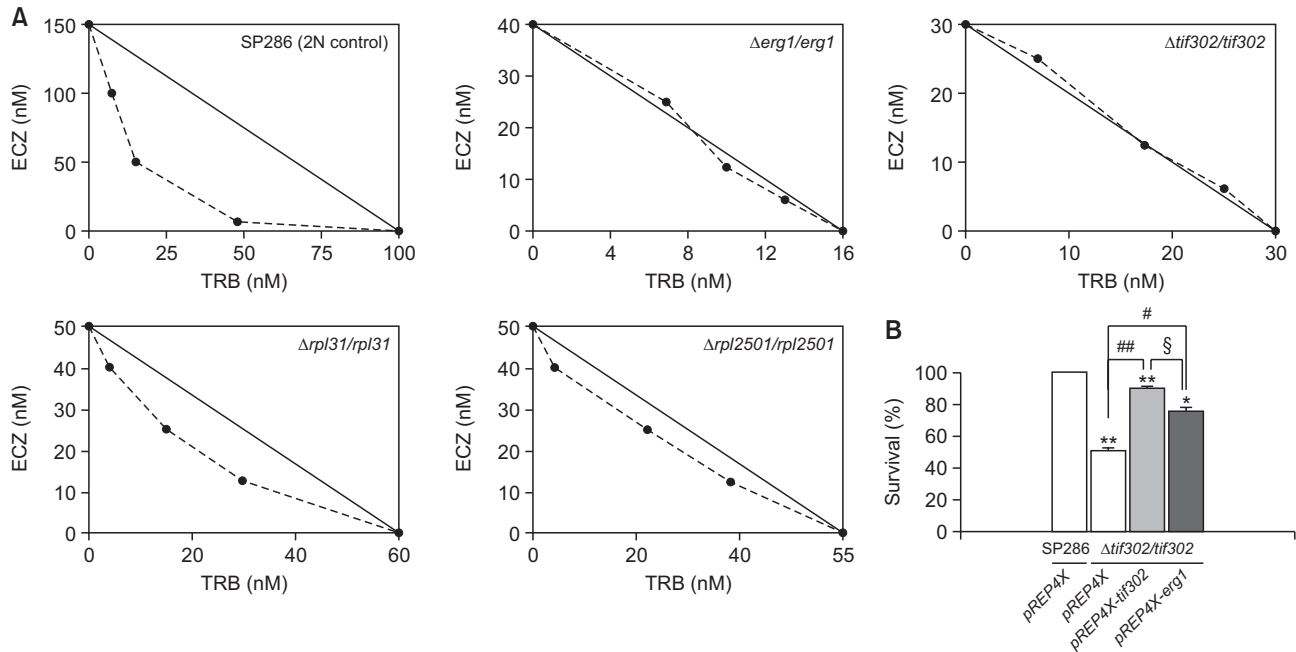
Fig. 4. Drug-drug target interactions of the 4 heterozygous TRB target strains in response to the co-treatment with TRB and ECZ. (A) The isobologram analysis of the heterozygous strains corresponding to the essential genes (*erg1*, *tif302*, *rpl31*, and *rpl2501*) was performed and their isobologram patterns were compared with that of the SP286 control. The abscissa and ordinate units (solid dots) correspond to the doses of TRB and ECZ. The downward concaves (dotted lines) and the diagonal lines represent the synergistic and additive effects, respectively. n=3; terbinafine (TRB) and econazole (ECZ). (B) Complementation of the *tif302* heterozygous strain by ectopic expression of the *tif302* or *erg1* gene. The *tif302* heterozygous strain was transformed with the expression plasmid pREP4X harboring the *tif302* (grey bar) or *erg1* (dark grey bar) gene. The growth fitness of the transformants was measured in the presence of TRB, and compared with that of the SP286 or *tif302* heterozygous strain (Δ*tif302/tif302*) harboring the vehicle (white bar). n=3; *$p<0.05$ or **$p<0.01$ vs. SP286; #$p<0.05$ or ##$p<0.01$ vs. *tif302* heterozygote; §$p<0.01$ vs. *tif302* heterozygote harboring the ectopic *tif302* gene.

the roles of RPs should work as components of repressor complexes for *erg1* transcription.

Among the 3 novel heterozygous target strains of essential genes, the Erg1 level of the *tif302* strain is the most similar to that of the *erg1* strain, based on the isobologram pattern

We identified, for the first time, 3 novel essential genes (*tif302*, *rpl2501*, and *rpl31*), besides the well-known *erg1* essential gene, as TRB target genes in fission yeast. As a measure to elucidate their action mechanisms, we employed isobologram analyses with the 4 heterozygous (*rpl31*, *rpl2501*, *tif302*, and *erg1*) and the SP286 control strain, as the isobologram graph pattern represents the relationship of drug-drug target interactions (Chou, 2006) (Fig. 4A).

First, SP286 was co-treated with a pair of ergosterol-targeting antifungals, TRB and ECZ, to expect a synergy via positive effects (Cavalheiro *et al*., 2009), because the TRB target (Erg1) precedes the ECZ target (Erg11) in the same ergosterol synthesis pathway. Expectedly, the isobologram pattern of SP286 showed the synergistic effects in response to the co-treatment with TRB and ECZ (on top of Fig. 4A). In contrast, the *rpl31* and *rpl2501* heterozygous strains showed decreased extents of synergy. Intriguingly, the *tif302* and *erg1* heterozygous strains showed the additive effects without synergy at all. Based on the isobologram patterns, the synergic effects of the heterozygous strains showed a descending trend as follows, SP286>*rpl31*≥*rpl2501*>*tif302*≅*erg1*. Notably,

the IC$_{50}$ values of TRB and ECZ in each heterozygous strain (16-60 and 30-50 nM) were decreased as represented by the *x*- and *y*-axis, compared with those of SP286 (100 and 150 nM). Probably, the synergic effects were associated with Erg1 levels. In this regard, the synergy disappeared in the *tif302* and *erg1* heterozygous strains, because their Erg1 levels decreased too much to affect Erg11 enzyme for the synergic effect. The results suggest that the Erg1 level of the *tif302* heterozygous strain was comparable with that of the *erg1* heterozygous strain, although the Erg1 levels of the 4 heterozygous strains were lower than in the SP286 control strain. Consistently, the squalene levels, as the secondary readout of Erg1 levels, were comparable between the *erg1* and *tif302* heterozygous strains, as shown in Fig. 1B.

However, it was hard to speculate how Tif302 could affect the cellular levels of *erg1* mRNA or Erg1 protein. Thus, we confirmed again whether the decreased Erg1 levels in the *tif302* heterozygous strain could be complemented by a gain-of-function experiment (Fig. 4B). When the *erg1* or *tif302* gene was overexpressed by the pREP4X plasmid in the *tif302* heterozygous strain, its TRB susceptibility was significantly ($p<0.05$) recovered, compared with the vehicle plasmid only. Notably, the complementation effects of *tif302* itself was significantly ($p<0.05$) superior to those of *erg1*. The results imply that TRB susceptibility of the *tif302* heterozygous strain may be attributed to an extra action mechanism, in addition to the decreased level of *erg1* mRNA.
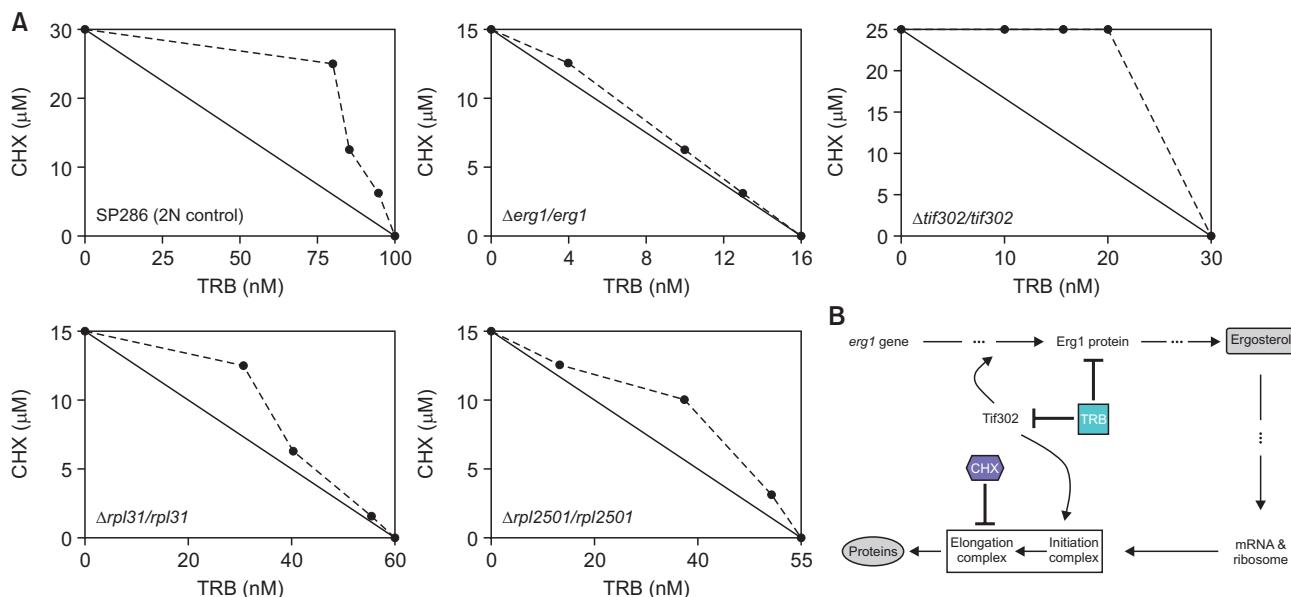
Fig. 5. Drug-drug target interactions of the 4 heterozygous TRB target strains in response to the co-treatment with TRB and cycloheximide and a proposed action mechanism based on their isobologram patterns. (A) The isobologram analysis of the heterozygous strains corresponding to the essential genes (*erg1*, *tif302*, *rpl31*, and *rpl2501*) was performed and their isobologram patterns were compared with that of the SP286 control. The abscissa and ordinate units (solid dots) correspond to the doses of TRB and CHX. The upward convex (dotted lines) and the diagonal lines represent the antagonistic and additive effects, respectively. *n*=3; terbinafine (TRB) and cycloheximide (CHX). (B) The proposed action mechanism of TRB and CHX. The model was proposed to explain the antagonistic effects of the isobologram pattern. Notably, Tif302 can be inhibited by TRB and its inhibition subsequently affects the protein translation process, which overlaps with the action mechanism of CHX.

The Tif302 protein is required for efficacy of both TRB and CHX

As all the heterozygous TRB target strains showed higher susceptibility to CHX compared with the SP286 control cells (Fig. 1C), CHX is likely to be related with modulation of ergosterol levels. In this regard, the strains were co-treated with TRB and CHX to gain more insight on the action mechanism of *tif302*. In principle, the expected isobologram effects would be additive or synergic, because the TRB target (Erg1) is not related with CHX target (elongation step of translation) (Schneider-Poetsch *et al*., 2010). Surprisingly, SP286 and the 4 heterozygous target strains showed the peculiar antagonistic effects at the rank of *tif302*>SP286>*rpl31*≅*rpl2501*>*erg1* (Fig. 5A).

To explain the serendipitous antagonistic effects, the action points of the 2 antifungals should be overlapping at least at a single point. As shown in the proposed model (Fig. 5B), Tif302 should be an overlapping point required for efficacy of both antifungals, as judged by the following findings. (i) All the heterozygous TRB target strains showed higher susceptibility to CHX compared with the SP286 control cells (Fig. 1C). The IC_{50} values of CHX decreased to 15-25 μM from 30 μM in SP286, as shown in the y-axis in the isobologram graphs. The lower levels of Erg1 made cells more vulnerable to stress (Bhattacharya *et al*., 2018), and in turn, more susceptible to CHX via synergic effects. (ii) The antagonistic effect consistently decreased with decreased levels of Erg1, as shown in the *erg1*, *rpl31*, and *rpl2501* heterozygous strains. (iii) However, the *tif302* heterozygous strain showed increased antagonism, even with Erg1 at levels comparable to the *erg1* heterozygous strain. This unexpected finding suggests that the Tif302 pro-

tein could be an overlapping point required for the efficacy of both TRB and CHX. As the initiation complex is a prerequisite for the elongation complex in the same ribosome complex (Jackson *et al*., 2010), the 2 sequential processes would be considered as a single process. To our knowledge, this is the first serendipitous finding to imply that TRB can have an extra target, Tif302, in addition to the well-known Erg1 enzyme.

TRB can bind to Tif302 via direct interaction

The above findings prompted us to assess whether TRB directly interacts with the Tif302 protein by the method of molecular modeling (Fig. 6, see Supplementary Fig. 1 and 2, and Supplementary Table 3 for more details). Regarding Erg1, TRB was found to bind to the 2 yeast Erg1 proteins with a binding energy of <–7 kcal/mol, which was lower than the –3.73 kcal/mol of the human SQLE protein (human ortholog of yeast Erg1). Based on the recent finding that human SQLE is a partial TRB target with a higher binding energy of –3.73 kcal/mol that the <–7.5 kcal/mol of yeast Erg1 (i.e.>1,000-fold higher IC_{50} than yeast Erg1) (Nowosielski *et al*., 2011; Padyana *et al*., 2019), yeast Tif302 should be a TRB target too because of the lower binding energy of –4.38 kcal/mol compared to –3.73 kcal/mol of human SQLE.

If TRB binds to Tif302, TRB treatment would affect the translation yield in a dose-dependent manner. Thus, we measured the translation yields in response to TRB treatment using GST as a reporter in wheat germ extracts (Supplementary Fig. 3). Expectedly, TRB treatment inhibited the *in vitro* translation of the GST reporter by 64% in a dose-dependent manner with a dose ranging from 20 to 2,000 nM TRB.

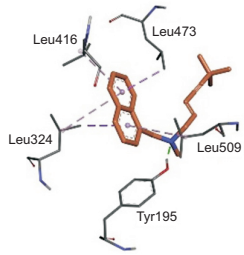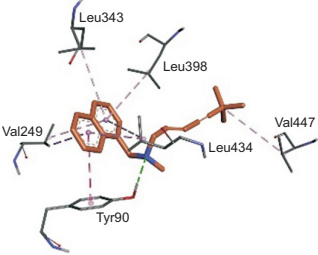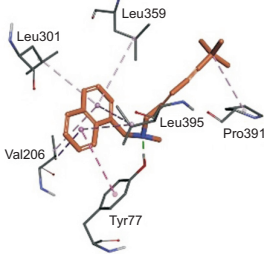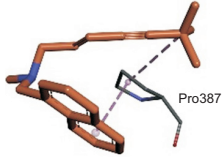Overall, TRB has a secondary off-target of fission yeast
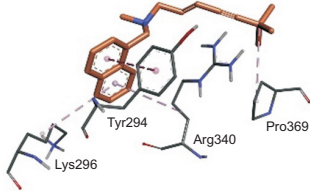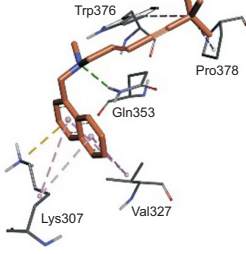
Target \ Organism	Human	Budding yeast	Fission yeast
Erg1			
Ortholog [binding energy (kcal/mol)]	SQLE (−3.73)	Erg1p (−7.51)	Erg1 (−7.57)
Tif302			
Ortholog [binding energy (kcal/mol)]	EIF3b (−2.33)	Prt1p (−4.24)	Tif302 (−4.38)

Fig. 6. Comparison of binding energy between terbinafine (TRB) and its target proteins including yeast Erg1 and Tif302, and their human orthologs. From the available crystal structures of the human SQLE, human EIF3B, and budding yeast Prt1p proteins, unknown protein structures of interest such as fission yeast Erg1 and Tif302 and budding yeast Erg1p were built via homology modelling. The binding energy between TRB and the indicated proteins was calculated through the generation of 3D affinity grid fields. TRB and residues in binding sites are represented using stick and slender models, respectively. Hydrogen bonds, hydrophobic-, and pi-sigma interactions are indicated as green, pink, and purple dashed lines, respectively (see supplementary material for more details).

Tif302, besides the conventional well-known Erg1 target. From the point of view of the off-target of Tif302, Tif302 can serve as a TRB target through 2 different action mechanisms, such as the decrease in *erg1* mRNA levels via an unknown mechanism, and the inhibition of translation yields via a direct binding to TRB.

A few of overlaps exist between TRB target genes screened from the heterozygous and haploid deletion libraries

As shown in Fig. 7, we compared the target genes of non-essential genes identified from the heterozygous deletion library in the study with those previously reported from the haploid deletion library (Fang *et al*., 2012). Notably, the comparison revealed a slight overlap. For example, dozens of target genes associated with the component, transport, and regulatory pathway in the ergosterol synthesis pathways were found only in haploid, but not in heterozygous strains. It is likely that the remaining copy out of a couple of target genes

is still functional in heterozygous strains. Conversely, some targets, such as the 7 RP genes, were only found from the heterozygous library, but not from the haploid library, because they could cause the opposite pattern of *erg1* mRNA levels, depending on ploidy. On the other hand, a few TRB targets, such as the SAGA subunit genes overlapped between the haploid and heterozygous libraries, because cellular amounts of co-activators could determine TRB susceptibility, depending on the concentration. Consistent with these results, several SAGA-subunit genes, including the *spt7* and *spt20* genes, have been reported to function as distinct subunits of SAGA co-activators for erg transcription in budding yeast (Hickman *et al*., 2011; Dewhurst-Maridor *et al*., 2017).

DISCUSSION

With technological advances in the field of genomics, yeast gene deletion libraries (Winzeler *et al*., 1999; Kim *et al*.,
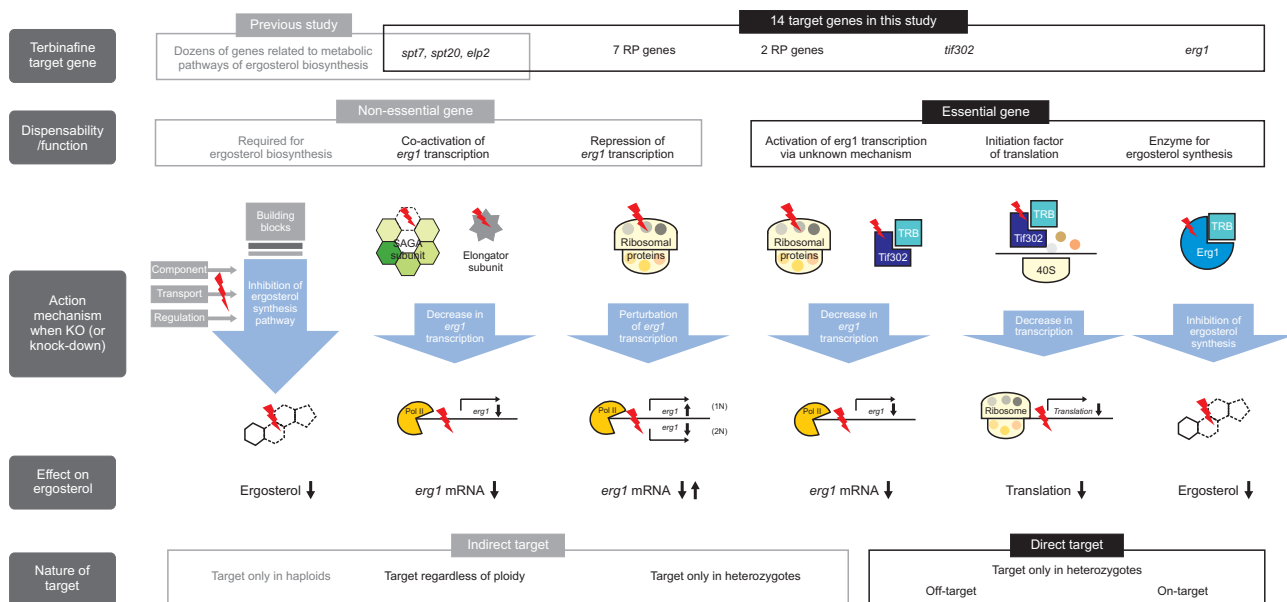
Fig. 7. Overview of action mechanisms of all the terbinafine (TRB) target genes screened so far. The action mechanisms of the 14 TRB target genes revealed from the heterozygous library in this study are illustrated along with those of non-essential target genes previously reported (Fang *et al*., 2012). Notably, Tif302 can serve as a potential secondary off-target of TRB.

2010) have become available for identifying target genes affected under any conditions of interest. In this study, for the first time, we screened TRB target genes in fission yeast from the heterozygous gene deletion library covering nearly all essential genes as well as non-essential genes. Compared with those reported from the haploid gene deletion library (Fang *et al*., 2012), we identified the novel target strains corresponding to the essential *tif302* gene, as well as non-essential RP and SAGA-subunit genes. To the end, we elucidated the action mechanisms of the novel target genes through in-depth functional analysis and presented the results as an illustrated overview (Fig. 7).

Compared with the previous study with the haploid gene deletion library (Fang *et al*., 2012), the asset of this study is that we found novel targets of essential genes. To our knowledge, we suggest for the first time that Tif302 would be a potential off-target of TRB, besides the primary on-target Erg1, through the serendipitous finding of the antagonistic effects in the isobologram analysis with TRB and CHX. In fact, the same drug-drug interaction analysis was tried with the budding yeast library, but they failed to find the antagonistic effects (Cokol *et al*., 2011). Probably, it was inadequate for them to find the antagonistic effects in budding yeast because the higher dose of TRB might prevent the systematic isobologram analyses from being properly interpreted. Indeed, TRB susceptibility of fission yeast is 350 times as high as that of budding yeast (fission vs. budding yeast=0.007-0.03 vs. 2.5-10.5 µg/mL in liquid media) (Lum *et al*., 2004; Cokol *et al*., 2011). Without question, the higher TRB susceptibility of fission yeast should be attributed to a higher penetration yield of TRB across the cell wall, because the Erg1 enzyme of 2 yeasts showed almost the same binding energy to TRB based on the molecular modeling analysis, as shown in Fig. 6. On the other hand, for the first time, we found that knockdown of *tif302* could down-regulate *erg1* mRNA levels, as shown in *tif302* heterozygous

strain (Fig. 1A). However, it was hard to speculate the underlying mechanism. As a clue, EIF3 (human ortholog of Tif302) has been reported to guide proliferation-related mRNAs into the ribosome, leading to translational activation or repression, similarly to transcriptional mediators (Lee *et al*., 2015). As the levels of *erg1* mRNA were proportional to the copy number of *tif302*, depending on ploidy, it would be a plausible explanation that the *tif302* gene product plays a role in preventing *erg1* mRNA from degradation, via an unknown mechanism. In this case, Tif302 could probably be associated with a protection of the *erg1* mRNA degradation via guidance of *erg1* mRNA to the ribosome.

These novel findings shed light on some aspects of the antifungal roles of Tif302. First, Tif302 would be considered as a potential antifungal target, as its inhibition by TRB affected the translation yield (Supplementary Fig. 3). Consistently, there is an accumulating body of evidence that EIF3B could be a potential anti-cancer target in human cancers (Wang *et al*., 2013; Xu *et al*., 2016; Ma *et al*., 2019). Next, according to our data, Tif302 would be a substitute target of CHX, because its inhibition by TRB offsets some efficacy of CHX, as shown in Fig. 5B.

In addition, we observed an unexpected phenomenon that non-essential RP genes are TRB targets only in heterozygous, but not in haploid, deletion strains, as shown in Fig. 3. Based on the comparison of the experimental ratio of *erg1* mRNA in the test strains, we propose a reasonable model for the action mechanism. According to the model (Fig. 3), RPs can modulate transcription levels of *erg1* mRNA by acting as components of repressor complexes. In agreement with the proposed model, there are many studies supporting that RPs play an extra role in transcriptional regulation, in addition to their classical role in ribosome assembly (Torres *et al*., 2001; Warner and McIntosh, 2009; Zhou *et al*., 2013, 2015). If this is the case, the repressor model of RPs as components can ex-

plain why many RP genes have been identified as multi-drug targets from screenings of the heterozygous library (Han *et al*., 2013). Also, it would provide a clue of how diploid cells produce twice the amount of proteins as haploid cells, by solving the dilution effects due to an enlarged cell volume (de Godoy *et al*., 2008).

It is of note that all human orthologs of the heterozygous target genes have been reported to be associated with diverse human diseases, as shown in Table 1. Surprisingly, the human orthologs of the 5 RP-encoding genes screened in the present study are associated with the congenital erythroid aplasia DBA. Thus far, 21, including 19 RP genes, have been reported to be associated with human DBA via haploinsufficiency of RP genes caused by point mutations (Ulirsch *et al*., 2018). Based on our findings, DBA may be attributed to a haploinsufficiency of RP genes via a perturbation in sterol homeostasis. Consistently, the anabolic pathways of sterol and heme are closely related with each other, as they share a common synthetic pathway from acetyl-CoA to farnesyl pyrophosphate (Zhang *et al*., 2015). Moreover, the 10 TRB target genes showed abnormal morphologies (Table 1) when their loss-of-function was observed for several generations after spore germination of the haploid deletion mutants using microscopy (Hayles *et al*., 2013). In addition, the haploid deletion mutant of the non-essential RP genes showed twice the doubling time, compared with the haploid ED668 control cells (data not shown). These findings indicate that sterol metabolism is critical for cellular homeostasis, both in humans (Singh *et al*., 2013; Spann and Glass, 2013) and in yeasts (Bhattacharya *et al*., 2018; Rodrigues, 2018).

In this study, we have identified both essential and non-essential TRB target genes by the detection of gene-specific bar codes through microarrays. The detection method of bar codes is on upgrade from microarrays to next-generation sequencing, which will confer more accuracy to the screening system without bar code errors (Han *et al*., 2010; Lee *et al*., 2018). Overall, we provide a proof of concept of how this genome-wide screening system can be harnessed for the identification and characterization of target genes affected under any condition of interest.

CONFLICT OF INTEREST

There are no conflict of interest.

ACKNOWLEDGMENTS

REFERENCES

Bhattacharya, S., Esquivel, B. D. and White, T. C. (2018) Overexpression or deletion of ergosterol biosynthesis genes alters doubling time, response to stress agents, and drug susceptibility in Saccharomyces cerevisiae. *mBio* **9**, e01291-18.

Cavalheiro, A. S., Maboni, G., de Azevedo, M. I., Argenta, J. S., Pereira, D. I., Spader, T. B., Alves, S. H. and Santurio, J. M. (2009) *In vitro* activity of terbinafine combined with caspofungin and azoles against Pythium insidiosum. *Antimicrob. Agents Chemother.* **53**, 2136-2138.

Chou, T. C. (2006) Theoretical basis, experimental design, and computerized simulation of synergism and antagonism in drug combination studies. *Pharmacol. Rev.* **58**, 621-681.

Cohen, J. S., Srivastava, S., Farwell, K. D., Lu, H. M., Zeng, W., Lu, H., Chao, E. C. and Fatemi, A. (2015) ELP2 is a novel gene implicated in neurodevelopmental disabilities. *Am. J. Med. Genet. A* **167**, 1391-1395.

Cokol, M., Chua, H. N., Tasan, M., Mutlu, B., Weinstein, Z. B., Suzuki, Y., Nergiz, M. E., Costanzo, M., Baryshnikova, A., Giaever, G., Nislow, C., Myers, C. L., Andrews, B. J., Boone, C. and Roth, F. P. (2011) Systematic exploration of synergistic drug pairs. *Mol. Syst. Biol.* **7**, 544.

Darkes, M. J., Scott, L. J. and Goa, K. L. (2003) Terbinafine: a review of its use in onychomycosis in adults. *Am. J. Clin. Dermatol.* **4**, 39-65.

de Godoy, L. M. F., Olsen, J. V., Cox, J., Nielsen, M. L., Hubner, N. C., Frohlich, F., Walther, T. C. and Mann, M. (2008) Comprehensive mass-spectrometry-based proteome quantification of haploid versus diploid yeast. *Nature* **455**, 1251-1254.

Dewhurst-Maridor, G., Abegg, D., David, F. P. A., Rougemont, J., Scott, C. C., Adibekian, A. and Riezman, H. (2017) The SAGA complex, together with transcription factors and the endocytic protein Rvs167p, coordinates the reprofiling of gene expression in response to changes in sterol composition in Saccharomyces cerevisiae. *Mol. Biol. Cell* **28**, 2637-2649.

Doherty, L., Sheen, M. R., Vlachos, A., Choesmel, V., O'Donohue, M. F., Clinton, C., Schneider, H. E., Sieff, C. A., Newburger, P. E., Ball, S. E., Niewiadomska, E., Matysiak, M., Glader, B., Arceci, R. J., Farrar, J. E., Atsidaftos, E., Lipton, J. M., Gleizes, P. E. and Gazda, H. T. (2010) Ribosomal protein genes RPS10 and RPS26 are commonly mutated in Diamond-Blackfan anemia. *Am. J. Hum. Genet.* **86**, 222-228.

Dong, Z., Zhu, X., Li, Y., Gan, L., Chen, H., Zhang, W. and Sun, J. (2018) Oncogenomic analysis identifies novel biomarkers for tumor stage mycosis fungoides. *Medicine (Baltimore)* **97**, e10871.

Draptchinskaia, N., Gustavsson, P., Andersson, B., Pettersson, M., Willig, T. N., Dianzani, I., Ball, S., Tchernia, G., Klar, J., Matsson, H., Tentler, D., Mohandas, N., Carlsson, B. and Dahl, N. (1999) The gene encoding ribosomal protein S19 is mutated in Diamond-Blackfan anaemia. *Nat. Genet.* **21**, 169-175.

Fang, Y., Hu, L., Zhou, X., Jaiseng, W., Zhang, B., Takami, T. and Kuno, T. (2012) A genomewide screen in Schizosaccharomyces pombe for genes affecting the sensitivity of antifungal drugs that target ergosterol biosynthesis. *Antimicrob. Agents Chemother.* **56**, 1949-1959.

Farrar, J. E., Quarello, P., Fisher, R., O'Brien, K. A., Aspesi, A., Parrella, S., Henson, A. L., Seidel, N. E., Atsidaftos, E., Prakash, S., Bari, S., Garelli, E., Arceci, R. J., Dianzani, I., Ramenghi, U., Vlachos, A., Lipton, J. M., Bodine, D. M. and Ellis, S. R. (2014) Exploiting pre-rRNA processing in Diamond Blackfan anemia gene discovery and diagnosis. *Am. J. Hematol.* **89**, 985-991.

Gazda, H. T., Grabowska, A., Merida-Long, L. B., Latawiec, E., Schneider, H. E., Lipton, J. M., Vlachos, A., Atsidaftos, E., Ball, S. E., Orfali, K. A., Niewiadomska, E., Da Costa, L., Tchernia, G., Niemeyer, C., Meerpohl, J. J., Stahl, J., Schratt, G., Glader, B., Backer, K., Wong, C., Nathan, D. G., Beggs, A. H. and Sieff, C. A. (2006) Ribosomal protein S24 gene is mutated in Diamond-Blackfan anemia. *Am. J. Hum. Genet.* **79**, 1110-1118.

Giaever, G., Shoemaker, D. D., Jones, T. W., Liang, H., Winzeler, E. A., Astromoff, A. and Davis, R. W. (1999) Genomic profiling of drug sensitivities via induced haploinsufficiency. *Nat. Genet.* **21**, 278-283.

Gripp, K. W., Curry, C., Olney, A. H., Sandoval, C., Fisher, J., Chong, J. X., Genomics, U. W. C. f. M., Pilchman, L., Sahraoui, R., Sta-

bley, D. L. and Sol-Church, K. (2014) Diamond-Blackfan anemia with mandibulofacial dystostosis is heterogeneous, including the novel DBA genes TSR2 and RPS28. *Am. J. Med. Genet. A* **164A**, 2240-2249.

Han, S., Lee, M., Chang, H., Nam, M., Park, H. O., Kwak, Y. S., Ha, H. J., Kim, D., Hwang, S. O., Hoe, K. L. and Kim, D. U. (2013) Construction of the first compendium of chemical-genetic profiles in the fission yeast Schizosaccharomyces pombe and comparative compendium approach. *Biochem. Biophys. Res. Commun.* **436**, 613-618.

Han, T. X., Xu, X. Y., Zhang, M. J., Peng, X. and Du, L. L. (2010) Global fitness profiling of fission yeast deletion strains by barcode sequencing. *Genome Biol.* **11**, R60.

Hayles, J., Wood, V., Jeffery, L., Hoe, K. L., Kim, D. U., Park, H. O., Salas-Pino, S., Heichinger, C. and Nurse, P. (2013) A genome-wide resource of cell cycle and cell shape genes of fission yeast. *Open Biol.* **3**, 130053.

Hickman, M. J., Spatt, D. and Winston, F. (2011) The Hog1 mitogen-activated protein kinase mediates a hypoxic response in Saccharomyces cerevisiae. *Genetics* **188**, 325-338.

Housden, B. E., Muhar, M., Gemberling, M., Gersbach, C. A., Stainier, D. Y., Seydoux, G., Mohr, S. E., Zuber, J. and Perrimon, N. (2017) Loss-of-function genetic tools for animal models: cross-species and cross-platform differences. *Nat. Rev. Genet.* **18**, 24-40.

Ianiri, G. and Idnurm, A. (2015) Essential gene discovery in the basidiomycete Cryptococcus neoformans for antifungal drug target prioritization. *mBio* **6**, e02334-14.

Ito, Y., Hashimoto, K., Ohkura, N., Morikawa, H., Nishikawa, H., Tanaka, A., Furu, M., Ito, H., Fujii, T., Nomura, T., Yamazaki, S., Morita, A., Vignali, D. A., Kappler, J. W., Matsuda, S., Mimori, T., Sakaguchi, N. and Sakaguchi, S. (2014) Detection of T cell responses to a ubiquitous cellular protein in autoimmune disease. *Science* **346**, 363-368.

Jackson, R. J., Hellen, C. U. and Pestova, T. V. (2010) The mechanism of eukaryotic translation initiation and principles of its regulation. *Nat. Rev. Mol. Cell Biol.* **11**, 113-127.

Jallepalli, P. V. and Pellman, D. (2007) Cell biology. Aneuploidy in the balance. *Science* **317**, 904-905.

Kim, D. U., Hayles, J., Kim, D., Wood, V., Park, H. O., Won, M., Yoo, H. S., Duhig, T., Nam, M., Palmer, G., Han, S., Jeffery, L., Baek, S. T., Lee, H., Shim, Y. S., Lee, M., Kim, L., Heo, K. S., Noh, E. J., Lee, A. R., Jang, Y. J., Chung, K. S., Choi, S. J., Park, J. Y., Park, Y., Kim, H. M., Park, S. K., Park, H. J., Kang, E. J., Kim, H. B., Kang, H. S., Park, H. M., Kim, K., Song, K., Song, K. B., Nurse, P. and Hoe, K. L. (2010) Analysis of a genome-wide set of gene deletions in the fission yeast Schizosaccharomyces pombe. *Nat. Biotechnol.* **28**, 617-623.

Korach, K. S., Metzler, M. and McLachlan, J. A. (1978) Estrogenic activity *in vivo* and *in vitro* of some diethylstilbestrol metabolites and analogs. *Proc. Natl. Acad. Sci. U.S.A.* **75**, 468-471.

Kramer, R. and Cohen, D. (2004) Functional genomics to new drug targets. *Nat. Rev. Drug Discov.* **3**, 965-972.

Lee, A. S., Kranzusch, P. J. and Cate, J. H. (2015) eIF3 targets cell-proliferation messenger RNAs for translational activation or repression. *Nature* **522**, 111-114.

Lee, M., Choi, S. J., Han, S., Nam, M., Kim, D., Kim, D. U. and Hoe, K. L. (2018) Mutation analysis of synthetic DNA barcodes in a fission yeast gene deletion library by sanger sequencing. *Genomics Inform.* **16**, 22-29.

Lum, P. Y., Armour, C. D., Stepaniants, S. B., Cavet, G., Wolf, M. K., Butler, J. S., Hinshaw, J. C., Garnier, P., Prestwich, G. D., Leonardson, A., Garrett-Engele, P., Rush, C. M., Bard, M., Schimmack, G., Phillips, J. W., Roberts, C. J. and Shoemaker, D. D. (2004) Discovering modes of action for therapeutic compounds using a genome-wide screen of yeast heterozygotes. *Cell* **116**, 121-137.

Ma, F., Li, X., Ren, J., Guo, R., Li, Y., Liu, J., Sun, Y., Liu, Z., Jia, J. and Li, W. (2019) Downregulation of eukaryotic translation initiation factor 3b inhibited proliferation and metastasis of gastric cancer. *Cell Death Dis.* **10**, 623.

Mahoney, C. E., Pirman, D., Chubukov, V., Sleger, T., Hayes, S., Fan, Z. P., Allen, E. L., Chen, Y., Huang, L., Liu, M., Zhang, Y., McDonald, G., Narayanaswamy, R., Choe, S., Chen, Y., Gross, S.,

Cianchetta, G., Padyana, A. K., Murray, S., Liu, W., Marks, K. M., Murtie, J., Dorsch, M., Jin, S., Nagaraja, N., Biller, S. A., Roddy, T., Popovici-Muller, J. and Smolen, G. A. (2019) A chemical biology screen identifies a vulnerability of neuroendocrine cancer cells to SQLE inhibition. *Nat. Commun.* **10**, 96.

Mukhopadhyay, R., Ray, P. S., Arif, A., Brady, A. K., Kinter, M. and Fox, P. L. (2008) DAPK-ZIPK-L13a axis constitutes a negative-feedback module regulating inflammatory gene expression. *Mol. Cell* **32**, 371-382.

Nowosielski, M., Hoffmann, M., Wyrwicz, L. S., Stepniak, P., Plewczynski, D. M., Lazniewski, M., Ginalski, K. and Rychlewski, L. (2011) Detailed mechanism of squalene epoxidase inhibition by terbinafine. *J. Chem. Inf. Model.* **51**, 455-462.

Ostrosky-Zeichner, L., Casadevall, A., Galgiani, J. N., Odds, F. C. and Rex, J. H. (2010) An insight into the antifungal pipeline: selected new molecules and beyond. *Nat. Rev. Drug Discov.* **9**, 719-727.

Padyana, A. K., Gross, S., Jin, L., Cianchetta, G., Narayanaswamy, R., Wang, F., Wang, R., Fang, C., Lv, X., Biller, S. A., Dang, L., Mahoney, C. E., Nagaraja, N., Pirman, D., Sui, Z., Popovici-Muller, J. and Smolen, G. A. (2019) Structure and inhibition mechanism of the catalytic domain of human squalene epoxidase. *Nat. Commun.* **10**, 97.

Parsons, A. B., Lopez, A., Givoni, I. E., Williams, D. E., Gray, C. A., Porter, J., Chua, G., Sopko, R., Brost, R. L., Ho, C. H., Wang, J., Ketela, T., Brenner, C., Brill, J. A., Fernandez, G. E., Lorenz, T. C., Payne, G. S., Ishihara, S., Ohya, Y., Andrews, B., Hughes, T. R., Frey, B. J., Graham, T. R., Andersen, R. J. and Boone, C. (2006) Exploring the mode-of-action of bioactive compounds by chemical-genetic profiling in yeast. *Cell* **126**, 611-625.

Rancati, G., Moffat, J., Typas, A. and Pavelka, N. (2018) Emerging and evolving concepts in gene essentiality. *Nat. Rev. Genet.* **19**, 34-49.

Rodrigues, M. L. (2018) The Multifunctional fungal ergosterol. *mBio* **9**, e01755-18.

Ryder, N. S. (1992) Terbinafine: mode of action and properties of the squalene epoxidase inhibition. *Br. J. Dermatol.* **126 Suppl 39**, 2-7.

Ryder, N. S., Frank, I. and Dupont, M. C. (1986) Ergosterol biosynthesis inhibition by the thiocarbamate antifungal agents tolnaftate and tolciclate. *Antimicrob. Agents Chemother.* **29**, 858-860.

Schenone, M., Dancik, V., Wagner, B. K. and Clemons, P. A. (2013) Target identification and mechanism of action in chemical biology and drug discovery. *Nat. Chem. Biol.* **9**, 232-240.

Schneider-Poetsch, T., Ju, J., Eyler, D. E., Dang, Y., Bhat, S., Merrick, W. C., Green, R., Shen, B. and Liu, J. O. (2010) Inhibition of eukaryotic translation elongation by cycloheximide and lactimidomycin. *Nat. Chem. Biol.* **6**, 209-217.

Shalem, O., Sanjana, N. E., Hartenian, E., Shi, X., Scott, D. A., Mikkelson, T., Heckl, D., Ebert, B. L., Root, D. E., Doench, J. G. and Zhang, F. (2014) Genome-scale CRISPR-Cas9 knockout screening in human cells. *Science* **343**, 84-87.

Singh, P., Saxena, R., Srinivas, G., Pande, G. and Chattopadhyay, A. (2013) Cholesterol biosynthesis and homeostasis in regulation of the cell cycle. *PLoS ONE* **8**, e58833.

Sipiczki, M. (2000) Where does fission yeast sit on the tree of life? *Genome Biol.* **1**, REVIEWS1011.

Spann, N. J. and Glass, C. K. (2013) Sterols and oxysterols in immune cell function. *Nat. Immunol.* **14**, 893-900.

Sui, Z., Zhou, J., Cheng, Z. and Lu, P. (2015) Squalene epoxidase (SQLE) promotes the growth and migration of the hepatocellular carcinoma cells. *Tumour Biol.* **36**, 6173-6179.

Takami, T., Fang, Y., Zhou, X., Jaiseng, W., Ma, Y. and Kuno, T. (2012) A genetic and pharmacological analysis of isoprenoid pathway by LC-MS/MS in fission yeast. *PLoS ONE* **7**, e49004.

Takemasa, I., Kittaka, N., Hitora, T., Watanabe, M., Matsuo, E., Mizushima, T., Ikeda, M., Yamamoto, H., Sekimoto, M., Nishimura, O., Doki, Y. and Mori, M. (2012) Potential biological insights revealed by an integrated assessment of proteomic and transcriptomic data in human colorectal cancer. *Int. J. Oncol.* **40**, 551-559.

Torres, M., Condon, C., Balada, J. M., Squires, C. and Squires, C. L. (2001) Ribosomal protein S4 is a transcription factor with properties remarkably similar to NusA, a protein involved in both non-ribosomal and ribosomal RNA antitermination. *EMBO J.* **20**, 3811-3820.

Ulirsch, J. C., Verboon, J. M., Kazerounian, S., Guo, M. H., Yuan, D., Ludwig, L. S., Handsaker, R. E., Abdulhay, N. J., Fiorini, C., Genovese, G., Lim, E. T., Cheng, A., Cummings, B. B., Chao, K. R., Beggs, A. H., Genetti, C. A., Sieff, C. A., Newburger, P. E., Niewiadomska, E., Matysiak, M., Vlachos, A., Lipton, J. M., Atsidaftos, E., Glader, B., Narla, A., Gleizes, P. E., O'Donohue, M. F., Montel-Lehry, N., Amor, D. J., McCarroll, S. A., O'Donnell-Luria, A. H., Gupta, N., Gabriel, S. B., MacArthur, D. G., Lander, E. S., Lek, M., Da Costa, L., Nathan, D. G., Korostelev, A. A., Do, R., Sankaran, V. G. and Gazda, H. T. (2018) The genetic landscape of Diamond-Blackfan anemia. *Am. J. Hum. Genet.* **103**, 930-947.

Veitia, R. A. and Potier, M. C. (2015) Gene dosage imbalances: action, reaction, and models. *Trends Biochem. Sci.* **40**, 309-317.

Visconte, V., Przychodzen, B., Han, Y., Nawrocki, S. T., Thota, S., Kelly, K. R., Patel, B. J., Hirsch, C., Advani, A. S., Carraway, H. E., Sekeres, M. A., Maciejewski, J. P. and Carew, J. S. (2017) Complete mutational spectrum of the autophagy interactome: a novel class of tumor suppressor genes in myeloid neoplasms. *Leukemia* **31**, 505-510.

Wang, H., Ru, Y., Sanchez-Carbayo, M., Wang, X., Kieft, J. S. and Theodorescu, D. (2013) Translation initiation factor eIF3b expression in human cancer and its role in tumor growth and lung colonization. *Clin. Cancer Res.* **19**, 2850-2860.

Warner, J. R. and McIntosh, K. B. (2009) How common are extraribosomal functions of ribosomal proteins? *Mol. Cell* **34**, 3-11.

Weiss, R. L., Kukora, J. R. and Adams, J. (1975) The relationship between enzyme activity, cell geometry, and fitness in Saccharomyces cerevisiae. *Proc. Natl. Acad. Sci. U.S.A.* **72**, 794-798.

Winzeler, E. A., Shoemaker, D. D., Astromoff, A., Liang, H., Anderson, K., Andre, B., Bangham, R., Benito, R., Boeke, J. D., Bussey, H., Chu, A. M., Connelly, C., Davis, K., Dietrich, F., Dow, S. W., El Bakkoury, M., Foury, F., Friend, S. H., Gentalen, E., Giaever, G., Hegemann, J. H., Jones, T., Laub, M., Liao, H., Liebundguth, N., Lockhart, D. J., Lucau-Danila, A., Lussier, M., M'Rabet, N., Menard, P., Mittmann, M., Pai, C., Rebischung, C., Revuelta, J. L., Riles, L., Roberts, C. J., Ross-MacDonald, P., Scherens, B., Snyder, M., Sookhai-Mahadeo, S., Storms, R. K., Veronneau, S., Voet, M., Volckaert, G., Ward, T. R., Wysocki, R., Yen, G. S., Yu, K., Zimmermann, K., Philippsen, P., Johnston, M. and Davis, R. W. (1999) Functional characterization of the S. cerevisiae genome by gene deletion and parallel analysis. *Science* **285**, 901-906.

Xu, F., Xu, C. Z., Gu, J., Liu, X., Liu, R., Huang, E., Yuan, Y., Zhao, G., Jiang, J., Xu, C., Chu, Y., Lu, C. and Ge, D. (2016) Eukaryotic translation initiation factor 3B accelerates the progression of esophageal squamous cell carcinoma by activating beta-catenin signaling pathway. *Oncotarget* **7**, 43401-43411.

Zhang, Z., Li, C., Wu, F., Ma, R., Luan, J., Yang, F., Liu, W., Wang, L., Zhang, S., Liu, Y., Gu, J., Hua, W., Fan, M., Peng, H., Meng, X., Song, N., Bi, X., Gu, C., Zhang, Z., Huang, Q., Chen, L., Xiang, L., Xu, J., Zheng, Z. and Jiang, Z. (2015) Genomic variations of the mevalonate pathway in porokeratosis. *Elife* **4**, e06322.

Zhou, X., Hao, Q., Liao, J. M., Liao, P. and Lu, H. (2013) Ribosomal protein S14 negatively regulates c-Myc activity. *J. Biol. Chem.* **288**, 21793-21801.

Zhou, X., Liao, W. J., Liao, J. M., Liao, P. and Lu, H. (2015) Ribosomal proteins: functions beyond the ribosome. *J. Mol. Cell Biol.* **7**, 92-104.

Zinzalla, V., Stracka, D., Oppliger, W. and Hall, M. N. (2011) Activation of mTORC2 by association with the ribosome. *Cell* **144**, 757-768.

www.biomolther.org